AIAA JOURNAL
Vol. 49, No. 3, March 2011

Low-Speed Static Stall Suppression Using Steady and Pulsed Air-Jet Vortex Generators

Simon A. Prince* and Vahik Khodagolian†
City University London, London, England EC1V 0HB, United Kingdom

DOI: 10.2514/1.J050754

An experimental investigation was undertaken to assess the ability of low-momentum steady and unsteady air injection, using pitched and skewed air-jet vortex generators on a Royal Aircraft Establishment 9645 rotor section in a nominally two-dimensional flow, to suppress quasi-steady flow separation at low speeds ($0.07 < M < 0.12$). Results from this study show that unsteady blowing using air-jet vortex generators at a jet-to-freestream velocity ratio of 2.0 and pulsing frequencies equal to or above 50 Hz led to an ∼20% increase in $C_{N\max}$, while steady blowing with an equal amount of total mass flow as the unsteady case led only to an ∼5% increase. Similar results were confirmed with respect to the delay in drag and pitching-moment divergence. A correlation was found between aerofoil trailing-edge shedding frequency and maximum normal force enhancement, where a maximum normal force coefficient was obtained at a reduced pulsing frequency, $F+ \sim 0.6$, corresponding with the natural shedding frequency of the aerofoil in stall. Tufts applied to the upper surface of the aerofoil highlighted interesting periodic wavelike motions of the separated area downstream of the air-jet orifices at low frequencies below ∼10 Hz, and they showed that the advance and retreat of the separated region was in synchronization with the activation and deactivation of the air jets during each pulse. The oscillations increased with increasing jet pulsing frequency until no wavelike motion could be detected.

Nomenclature

c	=	chord length, m
C_D	=	drag coefficient based on chord
C_M	=	pitching-moment (about quarter chord) coefficient based on chord
C_N	=	normal force coefficient based on chord
C_T	=	tangential force coefficient based on chord
Cp	=	pressure coefficient
C_μ	=	jet blowing momentum coefficient based on planform area (mean rms value for pulsed jet case)
DC	=	duty cycle, %
f	=	pulsing frequency, Hz
f_w	=	Jones wake function
F^+	=	nondimensional pulsing frequency, fL/U
H	=	total pressure, Pa
L	=	reference length (between air-jet orifices and aerofoil trailing edge), m
p	=	static pressure, Pa or psi
Re	=	Reynolds number
U	=	tunnel (freestream) flow speed, m/s
v	=	jet exit velocity, m/s
x	=	chordwise coordinate from leading edge, m
y	=	chord normal coordinate, m
z	=	spanwise coordinate, m
α	=	angle of attack, °
δ	=	boundary-layer thickness, m
ϕ	=	jet orifice skew angle with reference to local freestream flow, °
ψ	=	jet orifice pitch angle with reference to local surface tangent, °

Subscripts

c	=	based on chord
j	=	jet
l	=	local condition
max	=	maximum magnitude
min	=	minimum magnitude
t	=	trailing edge
∞	=	freestream

I. Introduction

THE suppression of upper-surface boundary-layer separation from wings and rotor blades and the resulting suppression, or delay to higher angle of attack, of subsequent stall has long been a goal of aerodynamics research. Flow control methods using geometrical modifications, such as leading-edge slats and slots, leading-edge droop, leading-edge rotation, and dynamically deforming geometries have been investigated in the past. Fluidic active flow control has also been investigated, including boundary-layer suction, steady air-jet or tangential slot blowing, and boundary-layer transition control.

However, unsteady (oscillatory and pulsed) blowing through narrow slots or orifices located on the top surface of a wing or blade has been a recent primary focus of active flow control research and has been shown to be an effective method for delaying incompressible static and dynamic stall, primarily due to the reduced mass flow requirements (compared with steady blowing) and more effective unsteady interaction with the separated flow region.

Most of the previous work on unsteady blowing to suppress stall has been conducted using oscillatory air injection through narrow slots. Oscillatory or pulsed air injection through a spanwise narrow hole or inclined slot induces lateral shear layer roll up and the formation of either a series of discrete spanwise vortices (as shown in Fig. 1), which reenergize the boundary-layer and delay flow separation, or a series of large-scale turbulent coherent structures, which can deflect and reattach a fully separated flow.

The focus of this study is the investigation of the effectiveness of pulsed injection through an array of pitched and skewed orifices, or air-jet vortex generators (AJVGs), that are known to be effective in delaying and suppressing stall from an aerofoil section when operated under steady blowing conditions. Pulsed activation of such a system is likely to induce the formation of longitudinal vortices or

Received 6 August 2010; revision received 6 October 2010; accepted for publication 12 October 2010.

*Senior Lecturer, School of Engineering and Mathematical Sciences. Member AIAA.
†Research Assistant, School of Engineering and Mathematical Sciences.

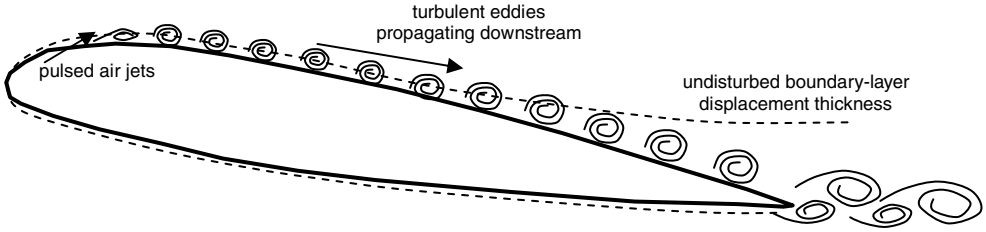

Fig. 1 Conceptual representation of the unsteady flowfield generated by leading-edge pulsed air-jet injection.

discrete turbulent eddies, depending on the pulsing frequency, which should reenergize the boundary layer in both spanwise and chordwise directions.

II. Review of Steady and Unsteady Air-Jet Flow Control for Separation Suppression

A. Steady Vortex-Generating Jet Flow Control

By artificially increasing the rate of fluid mixing within the boundary layer, one can increase the kinetic energy of the low-momentum near-wall fluid and thereby delay, or to some extent prevent, the onset of flow separation. Various flow control techniques, to reenergize boundary layers and suppress flow separation, have been identified and successfully tested, such as slot blowing, tangential blowing, and synthetic jets. The method of increasing fluid mixing rates by the artificial generation of near-surface longitudinal vortices has been found to be a particularly powerful technique. The vortices act to entrain high-energy flow from the undisturbed outer airstream and transport it into the low-momentum near-wall region deep inside the boundary layer. Mechanical, passive, vane vortex generators, first devised by Taylor and Hoadley [1], are the most common and widely used streamwise fluid vortex generators, and they commonly consist of thin solid strips fixed to the surface, usually located ahead of a separated flow region, at an angle to the oncoming flow. However, it has been shown that mechanical vane-type vortex generators impose an increase in drag caused by both the local pressure increase from flow blockage and by an increase in surface skin friction downstream of the device.

An alternative to passive solid vane-type vortex generators is an active fluid vortex-generating device, which was proposed by Wallis [2]. The idea is to use fluid injection via inclined and skewed (relative to the freestream flow vector) wall-bounded jets to induce longitudinal vortices for flow control instead of solid vane-type vortex generators. AJVGs usually consist of an array of small orifices embedded on a surface and supplied by a pressurized fluid source, wherein longitudinal vortices are induced by the interaction between the jets issuing from each orifice and the fluid flowing along the surface, as shown in Fig. 2. The orifices are pitched (angle ϕ in Fig. 2) with respect to the surface tangent and skewed (angle ψ in Fig. 2) with respect to the flow velocity vector over the surface. AJVGs do not induce as large a drag penalty as vane vortex generators and they can be actively operated and controlled, depending on the flow characteristics over a surface.

The early studies [3–9] identified the range of optimum jet orientations for maximum vorticity generation with steady blowing. Pearcey [3] and Freestone [4] showed that the optimum pitch angle for the strongest streamwise vortices is around $\phi = 30°$. The literature shows that the optimum skew angle is very sensitive, but it broadly lies in the range of $\psi = 45$ to $90°$. Selby et al. [7] identified an optimal skew angle between 60 and 90°, whereas Compton and Johnston [8] suggested a value between 45 and 90°. Henry and Pearcey [9] computed the turbulent flow over a flat plate with a single rectangular air jet, solving the Navier–Stokes equations with a simple algebraic turbulence model. A parametric study was performed, varying the slot aspect ratio between 1.0 and 5.0, the skew angle between 0 and 90, the pitch angle between 15 and 90°, and the jet velocity ratio (VR) between 0.5 and 2.0. The authors concluded that, in terms of the computed vortex strength and surface skin friction, where an increase in skin friction is desirable in this context, as it implies a thinning of the boundary layer and, hence, a healthier boundary layer to withstand separation, the optimum jet setting was a pitch angle of $\phi = 30°$ and a skew angle of $\psi = 60°$. Zhang and Collins [10,11] also showed that the optimum skew setting is in the range of 30 and 60° for effective flow control. Singh et al. [12,13] showed that the 30° pitch, 60° skew setting was, marginally, the most effective for stall suppression in experiments at low speeds on single-element aerofoils, and it was this orientation that was chosen for implementation in this study.

B. Oscillatory and Pulsed Air-Jet Flow Control

It is now understood that oscillatory or pulsed blowing for the suppression of boundary-layer separation is much more effective than pure steady blowing, and it has the additional benefit that much lower total mass flow levels are needed. The first exploratory study of unsteady blowing flow control on a wing section was by Oyler and Palmer [14], who developed an unsteady tangential blowing system

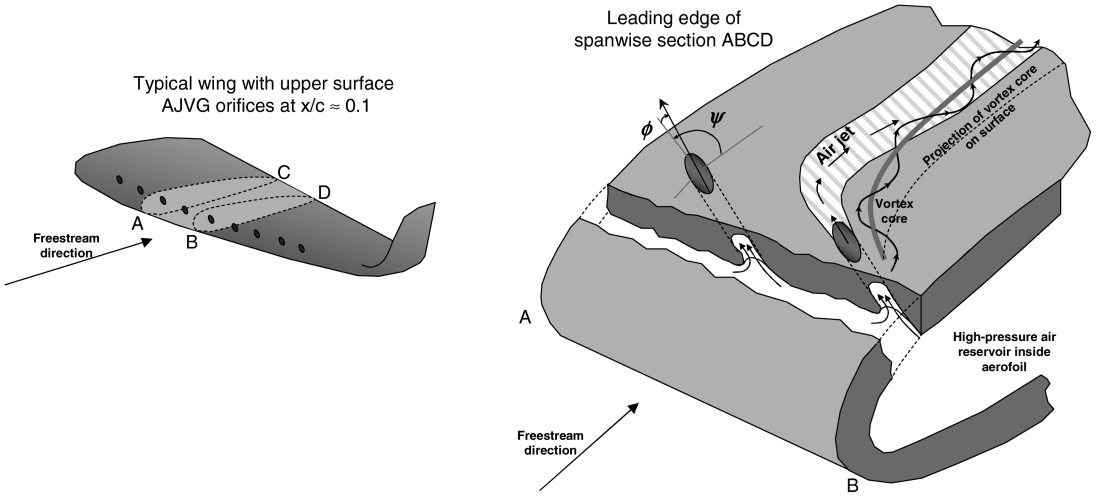

Fig. 2 Typical geometry of a leading-edge array of AJVGs with illustration of the physics of longitudinal vortex formation (after Pearcey [3]).

on a trailing-edge flap. Their experiments demonstrated a significant improvement of stall suppression and corresponding maximum lift capability, compared with steady blowing of equivalent total mass flow.

Oster et al. [15], Oster and Wygnanski [16], Wygnanski and Pedersen [17], and Ho and Huerre [18] conducted extensive fundamental studies of free turbulent mixing layers using artificial unsteady flow excitation (by means of mechanical oscillators), and they highlighted the complex flow physics and fluid dynamic benefits of introducing periodic disturbances to control the mixing in a fluid flow. Katz et al. [19] showed that a wall-bounded separated turbulent mixing layer could be attached to a curved surface by unsteady flow excitation, using a small vibrating ribbon to induce flow oscillations.

Seifert et al. [20] studied unsteady slot blowing on a multielement wing section comprising a NACA 0012 main wing with a trailing-edge flap. The experiments were performed under quasi-steady pitch conditions at Reynolds numbers, based on chord, between 10^5–10^6. The results showed that, for an order of magnitude less power consumption than required for steady blowing, unsteady blowing provided a significant increase in lift and a reduction of drag for angles of attack above which the unblown model was found to stall.

McManus et al. [21,22] successfully implemented unsteady oscillatory blowing AJVGs to suppress turbulent boundary-layer separation from a 20° ramp diffuser. The low-speed wind-tunnel tests were conducted at a Reynolds number based on the boundary-layer thickness at the jet exit δ_j of 2300. The AJVG array, located at $8\delta_j$ from the ramp shoulder, consisted of three circular jet orifices of diameter $0.67\delta_j$, spaced $4\delta_j$ apart, at a 45° pitch angle and a 90° skew angle relative to the oncoming freestream flow. Flow visualization using acetone vapor seeding and pulsed laser sheet illumination demonstrated that each pulse generated a large-scale vortical structure, which then convected downstream, keeping close to the ramp surface. The results of McManus et al. clearly demonstrated that, for a given total mass flow rate, oscillatory AJVGs were more effective in suppressing turbulent separation than steady blowing AJVGs. It also became clear that the mechanism of unsteady oscillatory or pulsed AJVG flow control is completely different to that of steady AJVG blowing. Under pulsed conditions, the jets do not generate the strong, continuous, streamwise vortices embedded within the turbulent boundary layer that are observed with steady AJVG air injection.

Unsteady fluid dynamic excitation is believed to induce the generation of large-scale turbulent coherent structures, particularly when the mean flow is unstable (as in a separated flow). The turbulent coherent structures act to entrain high-momentum freestream air and transport it into the low-momentum inner layers of the boundary layer, thereby enhancing turbulent mixing and suppressing separation.

Seifert et al. [23] undertook further studies on unsteady slot blowing from the upper surface of a trailing-edge flap linked with four different aerofoil section main elements. These low-speed experiments were performed at Reynolds numbers, based on chord, of between 0.15–1.2×10^6 and involved the parametric variation of the blowing frequency f. The results showed that the most effective blowing frequency occurred when reduced pulsing frequency was near unity.

McManus et al. [24,25] studied pulsed AJVG stall suppression on a stylized aerofoil section wing, where the 15.24 cm chord aerofoil comprised a leading-edge flat-plate flap and a flat-plate main section. The leading-edge section had a length of ~21% of the total chord of the model and was deflected down at 15° to the flat-plate main section. A zero angle of attack was thus defined as when the main section was at zero incidence to the freestream flow. The model incorporated a single circular orifice AJVG, of diameter $0.016c$, pitched at 45° and skewed at 90° to the local freestream flow. Low-speed wind-tunnel tests were performed at a Reynolds number, based on total chord, of 5.0×10^5. Jet-to-freestream VR (1.5–6.0), mass flow rate, and pulsing frequency (10–100 Hz) were varied to gain a better insight into their effect on stall suppression. The results of this study showed that the pulsed AJVG successfully delayed aerofoil stall from 12 to 16° angle of attack, and increasing VR and mass flow rate improved AJVG effectiveness. The results also showed that the optimum pulsing frequency is highly dependent on VR. When $\mathrm{VR} \leq 2$, the optimum reduced pulsing frequency was $F^+ \approx 0.5$, and for $\mathrm{VR} > 2$, optimum F^+ reduced to ~0.4. The study also pointed to the important result that the optimum pulsing frequency for separation control is achieved when it is the same as the natural shedding frequency of the eddies in the separated flow.

McManus and Magill [26,27] undertook an experimental study of pulsed AJVGs on a more realistic configuration: a two-element blade section comprising a NACA 4412 aerofoil main section and a leading-edge slat of 20% overall chord. The tests were performed across a Mach number range between 0.1 and 0.5. This study, again, highlighted the importance of jet VR. Optimum aerodynamic performance was found with $\mathrm{VR} = 7.4$ (maximum) and a pulsing frequency of $F^+ = 0.6$. The difference in F^+ between this study and McManus et al.'s earlier study [24] indicates that the optimum pulsing frequency is geometry dependent.

Greenblatt and Wygnanski [28] and Greenblatt et al. [29,30] performed a number of experiments on pulsed blowing, specifically for the control of dynamic stall. These experiments have demonstrated several consistent results, including the following:

1) The most effective location for unsteady forcing is near the point of separation.

2) The optimum reduced frequency for the oscillations is about $F^+ \approx 0.5$–1.0.

3) The amplitude of the oscillations required for effective separation control is about two orders of magnitude lower than that for steady blowing.

When oscillatory separation control is applied to an aerofoil that is not separated, the effects are not detrimental to lift. For dynamic pitching, prior work has shown that higher frequencies, typically ~200 Hz, are necessary, so that many pulses are produced during the pitchup. The effectiveness of the jets was found to generally increase with VR until a maximum effect was reached. Further increase in VR had no effect. Lift enhancement generally saturates in this way when the VR is increased beyond $\mathrm{VR} = 4$. Prior investigations also showed that duty cycles of 25% produce the same effect as those of 50% for a given VR. Thus, 25% is typically chosen, as it uses less air.

Eroglu and Breidental [31] investigated the flow structure when a pulsed jet of water was injected into a water flow, particularly focusing on the effect of pulsing frequency. It was shown that high-frequency pulsed blowing of jets in crossflow results in a flow very similar to steadily blown jets at the same blowing momentum coefficient. The time period between each injection of fluid mass was too short to allow the formation of coherent turbulent structures, and the individual pulses seemed to merge into a continuous stream, allowing the roll up of the streamwise boundary-layer-embedded vortices seen with steady AJVG blowing. Johari [32] made use of Eroglu and Breidental's [31] flow visualization data to propose a classification scheme for fully pulsed jets in crossflow based on the stroke ratio of the jet pulse and the duty cycle of the pulse train.

Scholz et al. [33] tested an array of pulsed air jets near the leading edge of a specially developed single-element aerofoil model designed to stall with an abrupt leading-edge separation. The experiments were performed in low-speed flow with a Reynolds number based on chord limited to 1.3×10^6. The spanwise array of 80 rectangular air jets, each with a length of $l/c = 0.125$ and an aspect ratio of 25, were skewed at 45° to the freestream flow. The array was tested at a chordwise location of 1% chord: first on the suction side, whereby the air jets were issuing directly into the separated region, and then at the same chordwise location on the pressure side, with the jets issuing into the turbulent boundary layer in between the attachment line and the separation line. It was found that with the jets positioned on the suction side, in the region of the separation line, they could not prevent separation. However, they were found to be able to increase the normal force coefficient above the prestall value by as much as 8%. The most sensitive parameter in this case was found to be the pulsed jet duty cycle, with the best results obtained with duty cycle in the range 12–25%. Pulsing frequency was not found to have a big effect in this case.

Ortmanns et al. [34] presented a study of the interaction of the turbulent coherent structures generated by a vortex-generating jet with a flat-plate turbulent boundary layer in a water tunnel with a maximum freestream speed of 2 m/s. The rectangular water jet orifice, with a dimension of 10×0.32 mm, was pitched at 90° and skewed at 45° to the freestream water flow. The authors used phase-locked stereoscopic particle image velocimetry to track the passage of the turbulent vortical structures as they passed downstream, varying the jet VR and the pulsing duty cycle. The pulsing frequency was fixed at 1 Hz. It was found that the velocity overshoot that occurred at the beginning of each pulse, which causes an enhanced mixing effect, is the most important factor in developing larger vortical structures with greater downstream impact. This startup effect was found to be sensitive to jet-to-freestream VR but generally independent of duty cycle. The downstream decay of the turbulent structures was also found to be independent of duty cycle.

In summary, the past work on oscillatory or pulsed AJVGs indicates that they represent a considerable improvement over steady AJVGs for the application of aeronautical flow control and, especially, stall suppression. Separation control using oscillatory blowing involves two different aspects: first is the delay of flow separation, and second is the reattachment of a fully separated flow, which may require two different approaches, since the receptivity of the unforced flow to unsteady forcing is different.

III. Experimental Details

A. Wind-Tunnel Facility

The experiments were conducted in the City University London T2 low-speed closed-circuit wind tunnel. The Royal Aircraft Establishment (RAE) 9645 model was mounted vertically in its octagonal working section of the width 1.12 m, the height 0.81 m, and the length 1.68 m. The rear of the working section was vented to atmosphere, and flow quality improvement was achieved by two fine-meshed turbulence screens mounted before the settling chamber. The T2 wind tunnel had a Reynolds number capability of 3.1 million/m, with a maximum speed limit of 45 m/s. The tunnel was also equipped with a compressed air feed system, with regulator valves to feed four inlet pipes. The fluctuation of the freestream dynamic pressure in the tunnel working section was measured to be within 0.5% of the nominal value for a flow velocity of 35 m/s.

The experiments were performed using the computer-controlled model turntable, allowing continuous variation of pitch. Angle-of-attack changes were performed at a pitching rate of 1°/s, and all pressure data were taken 30 s after each 1° incremental change in order to ensure that there would be negligible effect of pitch rate. The maximum blockage in the tests was ∼15%, but automatic compensation of fan speed was used to maintain constant tunnel flow velocity in the working section as the model was pitched. Correction of surface pressure measurements was not deemed to be necessary, as the study was comparative.

B. Model Design Details

An RAE 9645 aerofoil section model of 480 mm chord was developed, of the same basic design as those used in the study of Singh [13]. The model, designed to be a representative spanwise section of a helicopter rotor blade, was made of Tufnol, manufactured using layers of laminates bonded together with high-quality thermosetting resins. The model was then assembled by integrating individual spanwise aerofoil sections and held together by three spanwise rods. Endplates were also fitted at the two sides of the model to maintain a nominally two-dimensional flow. These endplates, while preventing the formation of strong tip vortices, also worked to isolate the model from the tunnel wall boundary layer. A thin 3 mm strip of sand roughness was glued to the leading edge of the model to promote turbulent boundary-layer development from the leading edge.

An important design objective for the pulsed blowing flow control system was to achieve a sufficient amount of jet exit momentum for a range of input frequencies, with minimum pressure loss and frequency attenuation. Since oscillatory or pulsed excitation of an internal plenum chamber, used in a previous study [13], led to major pressure loss and frequency attenuation, it was decided to use individually controlled flow actuators placed as close to the jet exit as possible. For application to aircraft wings or helicopter rotor systems, the individually controlled air injectors would be beneficial, as it was expected that the optimum actuation frequency would be different at different spanwise locations and for different azimuthal blade angles. A pulsed injection (rather than oscillatory) strategy was chosen, as it was deemed to be the best approach to achieve accurate control of the generation of sharply defined individual vortical structures. The final design of the pulsed blowing system on the RAE 9645 wing model, shown in Fig. 3, included a common internal pressure-regulated plenum tube (component 1) feeding the air injectors (component 2), with the air exiting at the aerofoil surface through the air-jet orifice (component 4) via connecting tubes (component 3). Components 5 and 6 are cavities designed for future flow control experiments at the trailing edge.

The ideal aerodynamic design would be to have the air-jet injectors flush-mounted with the aerofoil surface; this would reduce the pressure losses and frequency attenuation. The limiting factor to achieve this design was the internal geometric space restrictions of the wind tunnel, thereby placing a limit on the maximum size of the air-jet actuator. However, the length and geometry of the tubes connecting the injector to the jet exit and the pressurized air supply was designed to avoid flow resonance, reduce the internal pressure loss, and keep flow frequency distortions to a minimum.

The RAE 9645 model was configured with a single spanwise array of AJVGs on the upper surface of the aerofoil, consisting of 15 pitched and skewed AJVGs with circular orifice geometries (Fig. 2) located at 12% chord, since past studies [1–13] have shown that AJVG orifices need to be well upstream to provide enough length for fully developed boundary-layer embedded vortices to form. The jet orifices had a diameter of 4.8 mm, compared with the local undisturbed boundary-layer thickness of ∼5 mm at $\alpha = 0°$. The spacing between orifice centers was 45 mm, which is in the range for an optimum spacing-to-orifice-diameter ratio of 6 to 10 [3,4]. They were pitched at 30° from the surface tangent and skewed at 60° with respect to the freestream direction. The pitch and skew angles used at the jet exits were arranged to induce corotating streamwise vortices with steady blowing, in which each individual jet formed a streamwise vortical flow structure over the aerofoil surface. The British Standard mass flow rate of jet air entering the model was measured using a BS orifice plate rig, as described in [13].

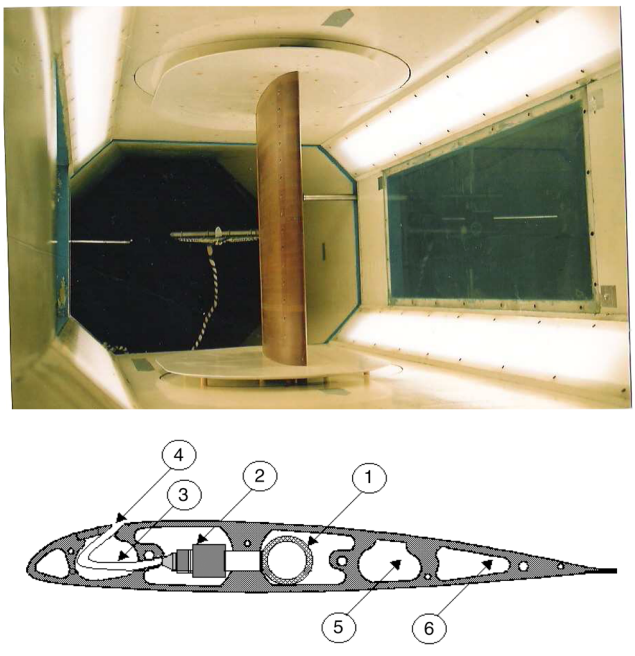

Fig. 3 RAE 9645 pulsed AJVG model and experimental setup.

Table 1 Performance of the electronically controlled high-speed jet actuator

Parameter	Value
Mass flow, g/s	$0.0 \leq \dot{m}_j \leq 3.665$
Supply pressure, psi	$0 < p \leq 30.0$
Pulsing frequency, Hz	$0.0 \leq f \leq 300.0$
Duty cycle (DC), %	$20.0 \leq \text{DC} \leq 100.0$

The model was instrumented with a total of 44 surface pressure tappings, positioned at the center span along the chord line, connected via short tubes to a 64-channel high-frequency electronic pressure scanner. An additional 18 surface pressure tappings were located downstream of one AJVG orifice.

C. Pulsed Air Injector

The pulsed air injector developed by Synerject, Inc., based on internal combustion engine solenoid fuel injector technology, was chosen as the pulsed air-jet actuator, since it was found to satisfy the required mass flow, pulsing characteristics, and geometrical size requirements. Table 1 provides details of the operating characteristics of the injector.

An electronic injector drive control unit was developed to enable individual or simultaneous activation and frequency control of each air injector and AJVG. A linear integrated circuit was designed to control and reduce the total input current required to open and hold the air injector valve. By holding the injector current at one-fourth of the peak current, power dissipation in the solenoid could be reduced by at least the same factor. Preliminary tests were conducted to assess the flow characteristics, including jet exit pressure, frequency, and the velocity of the jet. The jet flow characteristics were measured using a dynamic pressure transducer (Kulite CTQH-187, type B) installed at the jet exit (in the core region) to measure the pressure signal and frequency content of the air jet. The Kulite sensor was traversed laterally through the pulsing air jet to identify the jet core location, and dynamic pressure traces were recorded across the operating frequency range. The pressure traces were found to follow the sharp square-wave input signals very well up to 100 Hz. Above 10 Hz, there appeared an overshoot or spike in the pressure signal at the start of the pulse, similar to that described by Ortmanns et al. [34].

The air injectors could be operated in a steady or pulsed mode. Compressed air was supplied to a pressure-regulating valve and fed into the air injector intake. The pulsed output from the injector was fed through short connecting brass tubes to the jet exit. This bench test arrangement was identical to the one designed for the final RAE 9645 aerofoil model. The tests confirmed that the pressure signals measured at the air-jet orifices matched the sharp input electrical square-wave signals up to a pulsing frequency of 100 Hz. Beyond 100 Hz, the output pressure signals exhibited progressively more noise and less sharpness.

D. Measurement Details

Surface and wake pressures were recorded using a piezoelectric high-frequency pressure scanning system from Chell Systems, with a quoted accuracy of $\pm 0.1\%$ in the pressure range measured in this study. The surface pressure was measured via the chordwise array of 44 pressure tappings located on the centerline, and two other parallel lines of 18 pressure taps located 10 and 20 mm downspan on the upper surface, downstream of the AJVG array. These were introduced in order to measure any spanwise surface pressure variation induced by upwash and downwash flows of the longitudinal vortical structure. The pressures from these stations were used to obtain average pressure distributions with which to gain a better calculation, by integration of the measured pressure distributions, of the aerodynamic forces and moments. A previous study with a NACA 23012 model of 20% less chord length than the current model, but with similar density of pressure tappings, also involved the direct measurement forces and moments using a six-component force balance. This study was undertaken at a freestream velocity of 30 m/s: the highest speed for the model given the force limits on the balance. It was shown that the pressure integration technique, in this case, provided normal force values $\sim 5\%$ less than the measured value at 0° incidence; at the highest incidence of 18°, this discrepancy was only $\sim 2\%$. For tangential force, this discrepancy was 10 and 4%, and for pitching moment, it was 10 and 5%. The accuracy of the pressure integration method in this study is expected to by slightly better for the standard freestream velocity of 35 m/s. It is important to remember, however, that this is a comparative study, and these errors will follow the same trend and should be equivalent at the same incidence where data are compared at the same freestream velocity.

A wake rake was used to measure the aerofoil wake momentum deficit one chord length downstream of the aerofoil trailing edge. The wake rake consisted of 40 stainless-steel pitot probes and five static probes (outer diameter of 1.05 mm, and inner diameter of 0.81 mm). The pitot pressure probes were spaced at 7 mm intervals in the center and at 15 mm intervals toward each spanwise extremity, giving a total span of 350 mm. The static pressure tubes were used to measure any static pressure gradient across the wake. The angle of attack was measured using the electronic computer-controlled balance turntable with an accuracy of $\pm 0.2°$. Zero angle of attack was set using a laser mounted on the model chord line, for which the beam was centered on a vertical wire mounted on the turning vanes 5 m down the tunnel from the trailing edge. Measuring the pitot and static pressures across the wake, via the Chell high-speed pressure scanning system, permitted the calculation of the profile drag coefficient using Jones's method [35].

Before the tests, the velocity of the air jets were calibrated against the plenum pressure for the case of zero freestream tunnel flow. The effect of freestream flow would be to increase the jet velocity by a few percent. The average jet velocity was measured using a small pitot-static tube with a 2 mm outer diameter (0.4 times the jet orifice diameter) mounted to traverse the air jet.

The model is shown in Fig. 3, mounted in the T2 wind tunnel, together with the endplates and the wake rake, mounted from a manual three-axis arm-traverse system. Surface ultraviolet (UV) fluorescent tufts were also mounted in a grid system on the upper surface of the model during the last series of experiments. This simple surface flow technique allowed for the detection of surface flow features, such as separation lines, stall cells, and longitudinal vortices, and it could also resolve, for low frequency, their movement over time.

IV. Results and Discussion

A. Comparison of Steady and Pulsed Air-Jet Blowing

The first series of experiments involved the measurement of the surface pressure distributions on the RAE 9645 model with continuous angle-of-attack variation ($-10° < \alpha < 26°$) for a constant $U = 35$ m/s wind speed for the cases of 1) a clean surface model with the air-jet orifices smoothly sealed; 2) air-jet orifices open but inactive air jets; 3) steady air-jet blowing at VR = 0.5, 1.0, 1.5, and 2.0; 4) pulsed air-jet blowing at VR = 1.0, with pulsing frequency set at $f = 10$, 50, and 100 Hz; and 5) pulsed air-jet blowing at VR = 2.0, with pulsing frequency set at $f = 10$, 50, and 100 Hz. Comparison of the surface pressure distributions for both the sealed and open inactive air-jet cases showed that there was no detectable effect of open air-jet cavities on the surface pressures.

Examples of the surface pressure distributions measured for cases 1, 3, and 5 are plotted in Fig. 4 for $\alpha = 10$, 16, and 22°, respectively. At $\alpha = 10°$, before the occurrence of trailing-edge separation (C_{pt} still positive), there is no discernible difference, within the accuracy of pressure scanning equipment, between the six sets of data. At $\alpha = 16°$, the trailing-edge pressure coefficient is seen to be negative for the inactive blowing case, indicating that the boundary layer has separated over the rear upper surface. For all of the blowing cases, however, C_{pt} is seen to remain positive, indicating that all blowing cases are effective in suppressing trailing-edge separation at this angle of attack. Interestingly, both steady and pulsed air-jet blowing is seen to increase the level of suction over the forward 50% of the

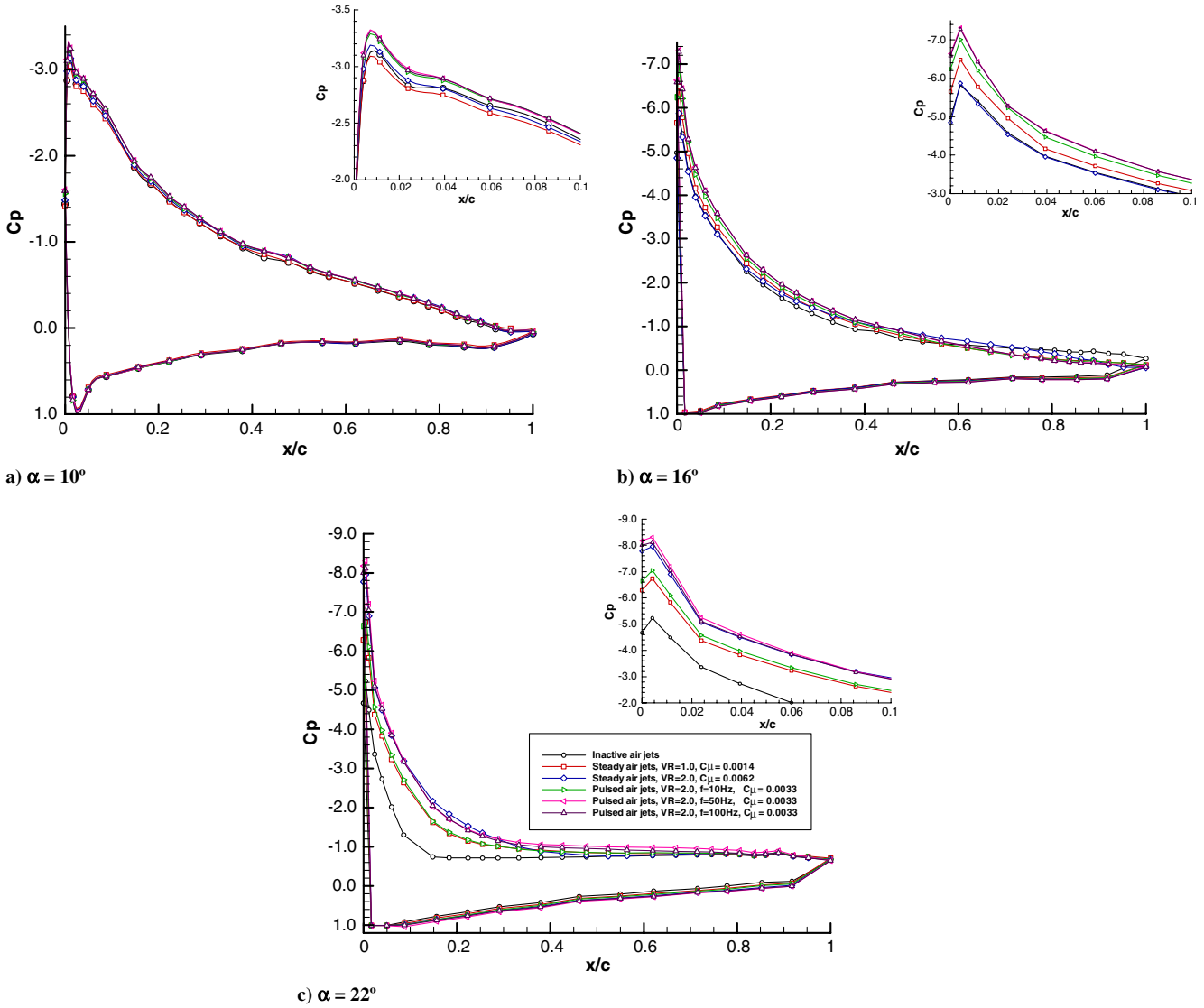

Fig. 4 Variation of centerline surface pressure distribution with steady and pulsed air-jet blowing at angles of attack of a) 10, b) 16, and c) 22° ($U = 35$ m/s and $Re_C = 1.1 \times 10^6$).

aerofoil upper surface, with the pulsed air-jet blowing at 100 Hz pulsing frequency clearly giving the greatest enhancement.

At $\alpha = 22°$, fully separated flow beyond ~10% chord is indicated for the inactive air-jet case by the pressure plateau. While the rearmost portions of the upper surface are seen to experience separated flow for all of the cases, air-jet blowing is clearly demonstrating a capability to defend the leading-edge suction against the upstream advance of the separation front, thereby delaying stall to higher angle of attack. Steady blowing at VR = 2.0 can clearly be seen to be outperforming VR = 1.0 steady blowing in maintaining high levels of leading-edge suction. Pulsed blowing at VR = 2.0 at the lowest $f = 10$ Hz pulsing frequency is seen to match the steady VR = 1.0 results, but an increase in pulsing frequency to 50 Hz results in performance almost equivalent to steady blowing at VR = 2.0. Given that the duty cycle for all of these experiments was set at a constant 50%, this is achieved with half the overall mass flow of the equivalent steady case. A further increase in pulsing frequency to $f = 100$ Hz is not seen to result in any further significant improvement.

Figure 5 provides a comparison of the effects of steady and pulsed AJVG blowing on the variation of aerodynamic characteristics with continuous variation angle of attack, starting from $\alpha = -10°$, increasing up to a maximum $\alpha = 26°$ (pitchup), and followed by a progressive reduction back down to $\alpha = -10°$ in steps of $\Delta\alpha = 1°$.

Figure 5a compares the results for the calculated variation of a normal force coefficient with the angle of attack. The C_N curve for steady blowing at VR = 1.0 does not appear to differ significantly from the unblown case until beyond $\alpha \sim 18°$. At higher incidences, steady blowing at VR = 1.0 is seen to prevent the sudden drop in C_N associated with the collapse of leading-edge suction and the onset of full stall all the way up to $\alpha = 25°$. At $\alpha = 26°$, the level drops down to the unblown level. Once the pitchdown began, C_N levels were initially found to plunge to a level some ~5% below those seen with no blowing before (between $\alpha = 21°$–$20°$), a significant recovery was seen bringing the C_N level back to its pitchup level for the same angle of attack. This pitch hysteresis in C_N is not observed in the data for the unblown model case. The addition of energy into the separated flow region by steady air-jet blowing clearly promotes the early recovery of attached flow on the leading edge. Close scrutiny of Fig. 5d shows that steady blowing at VR = 1.0 does not suppress the occurrence of incipient trailing-edge separation (C_{pt} drops to zero), which is seen to occur at between $\alpha = 11$ and 12°.

Increasing the blowing VR to 2.0 vastly improved the effectiveness of steady AJVG blowing. $C_{N\max}$ was increased from ~1.42 without air-jet blowing, to ~1.5 with steady blowing at VR = 1.0, up to ~1.76 with blowing at VR = 2.0. The increase in blowing jet VR is also seen to delay the onset of trailing-edge separation to about a 3.5° greater angle of attack. A small loss in C_N, resulting in a kink at about $\alpha = 15°$, with a further small increase in angle of attack, is then almost certainly due to the loss of surface suction on the rearmost upper surface as the separation front

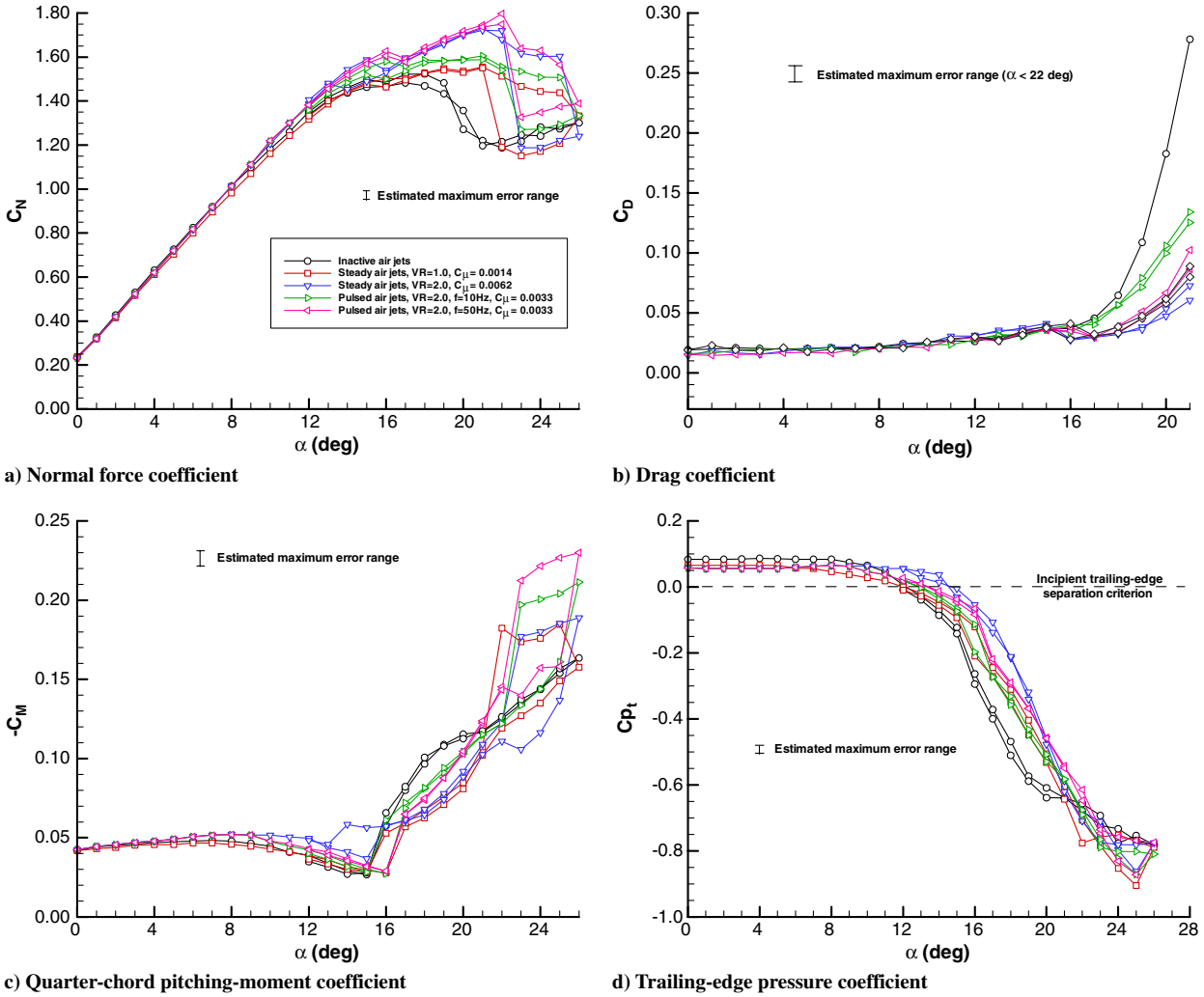

a) Normal force coefficient

b) Drag coefficient

c) Quarter-chord pitching-moment coefficient

d) Trailing-edge pressure coefficient

Fig. 5 Variation of C_N, C_M, C_D, and Cp_t with angle of attack for steady and pulsed air-jet blowing ($U = 35$ m/s and $Re_C = 1.1 \times 10^6$).

advances rapidly upstream. Steady blowing at VR = 2.0 is seen to deliver considerably higher normal force levels, beyond $C_{N\max}$, compared with steady VR = 1.0 blowing up to $\alpha = 25°$. A further pitchup to the maximum 26° angle of attack, however, results in a complete collapse of leading-edge suction, as with the VR = 1.0 case, but recovery on the pitchdown occurs at about a 1° angle of attack earlier, resulting in a return to $C_{N\max}$. Hysteresis is also evident in the occurrence of trailing-edge reattachment on the pitchdown, which takes place at about a 1° lower angle of attack.

Pulsed blowing at VR = 2.0 and $f = 10$ Hz resulted in a C_N characteristic on the pitchup very similar to that obtained with steady blowing at VR = 1.0 but with marginally increased levels (~3%) of normal force at a given angle of attack above the incipient trailing-edge separation angle. On the downstroke, however, pulsed blowing at VR = 2.0 and $f = 10$ Hz resulted in an initial drop in C_N to the same level as seen without any air-jet blowing and a recovery at the same angle of attack as observed with steady VR = 2.0 blowing. This indicates that pulsed air-jet blowing, even at a low 10 Hz frequency, is much more effective in enhancing mixing in, and reenergization, of a separated shear layer than steady air-jet blowing of equivalent jet-to-freestream VR.

An increase in the pulsing frequency from 10 to 50 Hz resulted in C_N characteristics almost identical to those seen with steady blowing at the same VR. Close examination reveals, however, that this 50 Hz pulsing case has a marginally higher $C_{N\max}$ of ~1.8, which the surface Cp measurements reveal is associated with slightly higher suctions on the front portions of the upper surface. Incipient trailing-edge separation with VR = 2.0 and 50 Hz pulsing is seen to occur at around $\alpha = 13°$, which is some 2° lower than with steady blowing at the same VR, indicating that pulsed air jets may not be quite as effective in delaying trailing-edge separation as steady blowing. However, significantly improved levels of C_N are seen at the beginning of the pitchdown with 50 Hz pulsing, which are nearly 10% higher than those calculated for either the unblown model or the 10 Hz pulsed blowing at VR = 2.0. Recovery to $C_{N\max}$ occurs at the same angle of attack on the pitchdown as was seen with the lower 10 Hz pulsing. Clearly, 50 Hz pulsing provides improved normal force characteristics over 10 Hz pulsing. The results for $f = 100$ Hz were found to be practically identical with those for 50 Hz and were therefore omitted for clarity.

For the case of VR = 2.0, the occurrence of pitch hysteresis between pitchup and pitchdown aerodynamic characteristics was observed with pulsed blowing at the same angle-of-attack ranges as seen with steady blowing. This is the case for all three pulsing frequencies of 10, 50, and 100 Hz.

Since the pulsed jet duty cycle is 50%, steady blowing at VR = 1.0 nominally delivers the same total mass flow rate as the pulsed jets operating at VR = 2.0, whatever pulsing frequency is employed. The results show that pulsed AJVGs are capable of delivering improved aerodynamic performance over steady AJVG blowing for the same total mass flow rate. This is, in part, due to the higher VR jet obtained for the same total mass flow of blown air that is enabled by pulsed blowing. Pulsed blowing is seen to give a $C_{N\max}$ of approximately 1.8, compared with a figure of approximately 1.5 for the corresponding steady blowing case: an improvement of 20%.

Figure 5b presents the variation of drag coefficient C_D (calculated by integration of the Jones wake function) with angle of attack for $U = 35$ m/s and jet blowing at VR = 2.0. Above $\alpha = 21°$, the viscous wake was seen to become too wide to be completely resolved by the wake rake, and data above this angle of attack have therefore

been omitted. In addition, separated flow and flow reversal induced an angular momentum component that could not be measured using the linear momentum deficit method. As angle of attack increases, the level of the underprediction of C_D will increase. The conclusions can, therefore, only be accurately drawn from the data below $\alpha = 21°$.

The experimental data presented in Fig. 5b show that the rapid divergence in C_D (beginning at $\alpha = 16°$) soon after trailing-edge separation for the inactive jet case is considerably suppressed by steady AJVG blowing at VR = 2.0 and pulsed AJVG blowing at VR = 2.0 for pulsing frequencies f of 10, 50, and 100 Hz. Pulsing at 10 Hz is seen to considerably reduce the drag coefficient for a given angle of attack between 17 and 21°, but the effect is perhaps only half as effective as steady blowing. Pulsing at 50 and 100 Hz, which seems to deliver almost identical behavior, provides almost the same level of suppression in drag divergence as steady blowing. For a given angle of attack, between 17 and 20°, the magnitude of C_D for $f = 50$ and 100 Hz is almost identical to the steady blowing result. This reveals that, for the same jet-to-freestream velocity, pulsed AJVG blowing at 50 and 100 Hz can provide a similar suppression of drag divergence as steady blowing but at only half the total blowing mass flow.

The data show the typical variation of C_D versus α for a turbulent case exhibiting no sign of any laminar drag bucket. One interesting feature is a sudden drop in the magnitude of C_D by as much as 30%, seen to occur soon after trailing-edge separation, before the beginning of a steady rise with angle of attack.

Similar behavior can be seen in the variation of the quarter-chord pitching moment with angle of attack (Fig. 5c). In contrast with the evidence from the steady blowing cases, the pulsed AJVG cases are seen to delay, by $\Delta\alpha = 1°$, the onset of the rise in pitching moment following trailing-edge separation. The subsequent magnitude of C_M for a given α up to $\alpha = 21°$ is seen to be consistently lower for the pulsed blowing cases than for the inactive jet case. The hysteresis in C_M, between pitchup and pitchdown, for $\alpha = 22$–$26°$ is observed, where the 50 Hz pulsing case is observed to cause a significantly higher value of C_M before the pitchdown. This is due to the maintenance of slightly higher levels of leading-edge suction for the 50 Hz pulsing case.

It is important to note that these results were found, within the limits of experimental and integration accuracy, to be repeatable, with three complete pitch sweeps having been performed. The clear differences between the results at $f = 10$ and 50 Hz are important clues, showing that whatever physical effect is occurring with pulsed AJVG blowing (an important change in physics) occurs between 10 and 50 Hz pulsing frequency.

B. Effect of Freestream Reynolds Number, VR = 1.75 and $f = 50$ Hz

The results of the experimental investigation of the effect of the freestream Reynolds number (based on model chord) is presented in Fig. 6 for pulsed AJVGs at VR = 1.75 and $f = 50$ Hz. The results show that, for a given angle of attack, there is very little discernible difference up to $\alpha = 20°$ within the limits of experimental

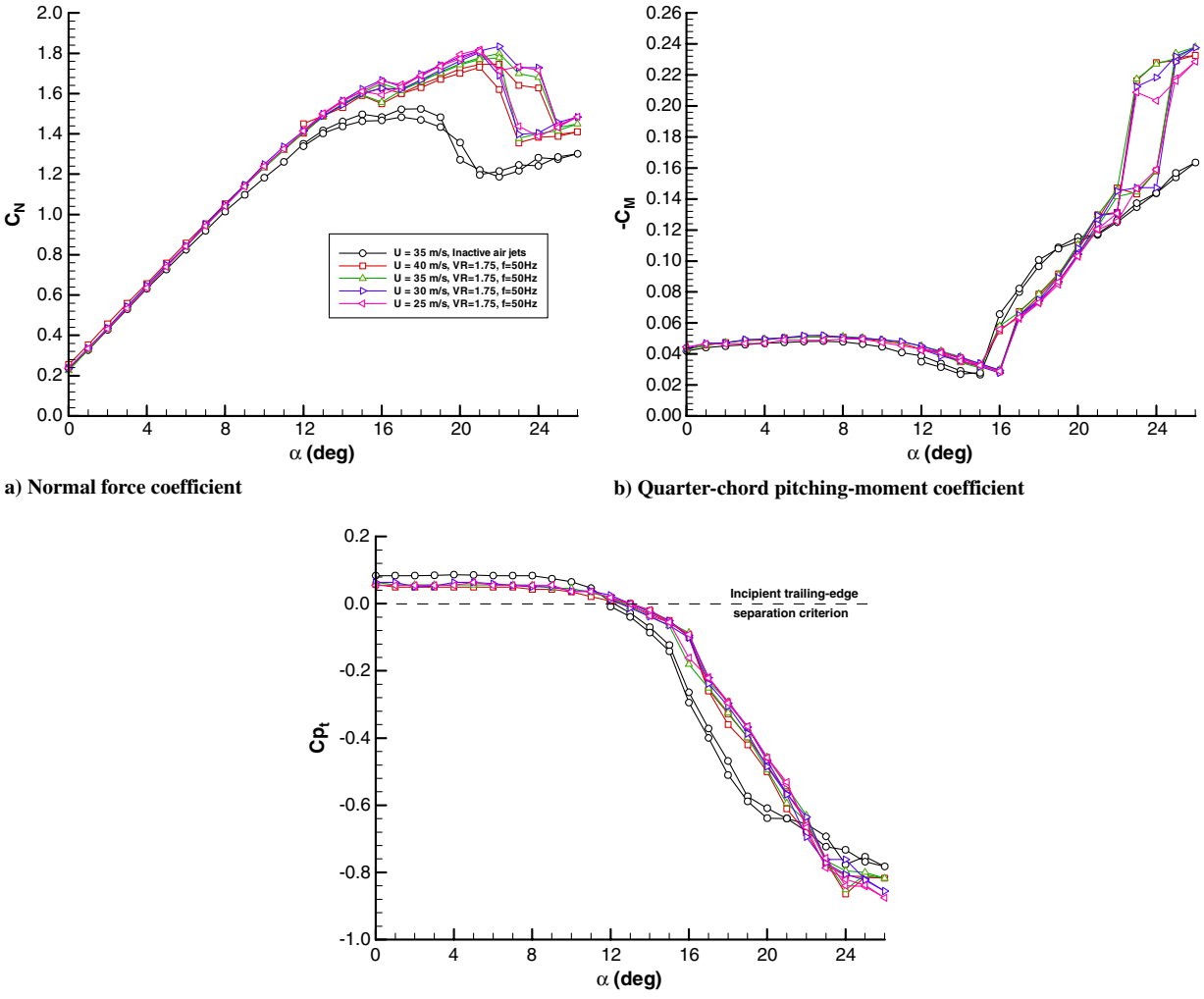

a) Normal force coefficient

b) Quarter-chord pitching-moment coefficient

c) Trailing-edge pressure coefficient

Fig. 6 Variation of C_N, C_M, and Cp_t with angle of attack for pulsed air-jet blowing, with varying freestream velocity at constant air-jet-to-freestream VR of 1.75 and pulsing frequency of $f = 50$ Hz.

accuracy in the values of C_N, C_M, and C_{pt} within the Reynolds number range:

$$Re_c = 0.79 \times 10^6 (U = 25 \text{ m/s}) – Re_c = 1.27 \times 10^6 (U = 40 \text{ m/s})$$

Above $\alpha = 20°$, there are small differences between the results on the pitchup, with the highest C_N and lowest C_M measured at the lowest freestream Reynolds number. No Reynolds number effects were discerned in the data for the inactive jet cases at different freestream velocities. These results are, of course, only valid across the limited Reynolds number range of $0.79 \times 10^6 < Re_c < 1.27 \times 10^6$. A further study is required, employing a wind tunnel, ideally, with a much higher speed capability to characterize the effect of the Reynolds number across a much greater and physically meaningful Reynolds number range.

C. Effect of Jet-to-Freestream-Velocity Ratio, $U = 25$ m/s and $f = 50$ Hz

Figure 7 presents the results of the experiments to highlight the effect of varying the jet-to-freestream VR (between 1.0 and 2.8) for a constant tunnel speed of $U = 25$ m/s and a constant pulsing frequency of 50 Hz. Incipient trailing-edge separation can clearly be seen (from Fig. 7c) to be strongly effected by an increase in jet VR. The results are summarized in Fig. 8, which presents the estimated (from C_{pt} versus α) variation of the angle of attack for incipient trailing-edge separation with jet-to-freestream VR.

The angle of attack for incipient trailing-edge separation, which is about 12° for the inactive jet case, is seen to be suppressed by the action of the pulsed AJVGs to a value estimated to be about 15.5° with VR = 2.8. The data for VR = 1.0 would suggest that, at this low jet VR, the effect at the trailing edge is minimal. A progressive increase in jet-to-freestream VR above 1.0 results in a progressive increase in the angle of attack required to cause trailing-edge separation.

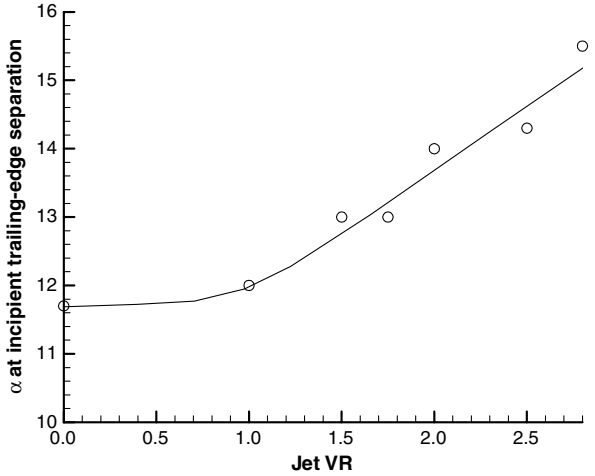

Fig. 8 The effect of jet-to-freestream VR on the angle of attack at incipient separation at the trailing edge ($U = 25$ m/s) and pulsing frequency of $f = 50$ Hz.

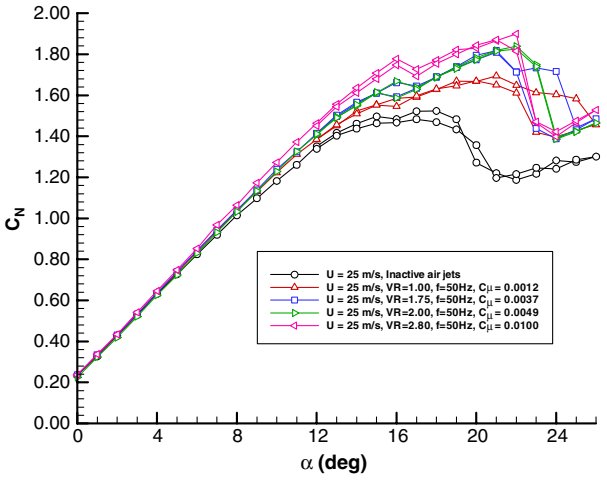

a) Normal force coefficient

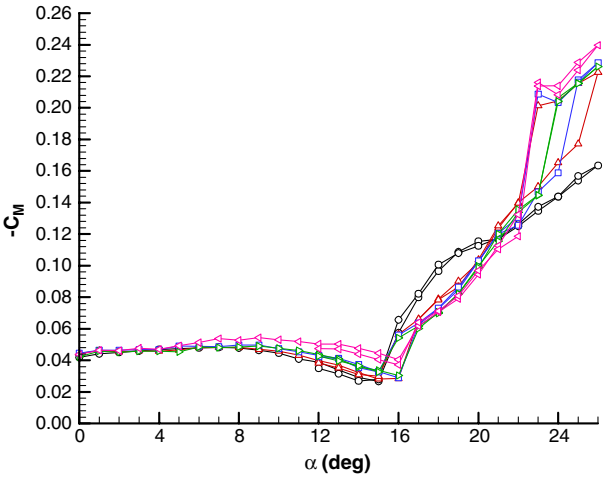

b) Quarter-chord pitching-moment coefficient

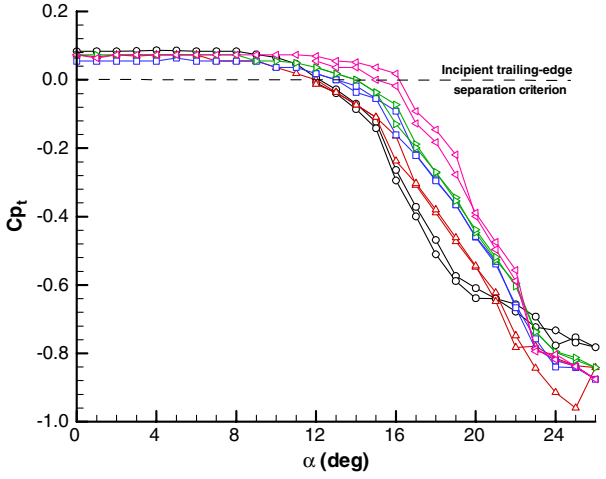

c) Trailing-edge pressure coefficient

Fig. 7 Variation of C_N, C_M, and Cp_t with angle of attack for pulsed air-jet blowing, with varying air-jet-to-freestream VR at constant freestream velocity of $U = 25$ m/s and pulsing frequency of $f = 50$ Hz.

Figure 7a, which plots the variation of C_N with α for the inactive jet case and compares this with data for four selected pulsed jet cases, presents a number of interesting findings. First, scrutiny of the curves in the vicinity of $\alpha = 16°$ reveals that the pitch hysteresis, between pitchup and pitchdown, associated with trailing-edge separation is not present in the data for VR = 2.8. This phenomenon, which is not evident in any of the inactive jet or clean aerofoil data, has been found in all of the data for steady and pulsed AJVG blowing at VR = 1.0 and 2.0, so far investigated. The data from this experiment confirm that hysteresis between the pitchup and pitchdown data occurs for jet-to-freestream VRs of 1.0, 1.5, 1.75, 2.0, and 2.5. For VR = 2.8, however, both of the experiments performed for this case reveal no similar hysteresis phenomenon.

Interestingly, the same finding holds true for the second hysteresis event, associated with the collapse and recovery of boundary-layer attachment on the forward 10% of the upper surface. For VR = 1.0–2.5, clear differences in the C_N and C_M data for pitchup and pitchdown are evident. For $VR = 2.8$, however, boundary-layer separation from the leading edge and the associated sudden loss of leading-edge suction occur at the same angle of attack ($\alpha = 22$–$23°$) on the pitchup as the recovery of the boundary-layer attachment and the leading-edge suction on the upper surface occurs on the pitchdown. It is expected that for VR > 2.8, the suppression of any hysteresis in aerodynamic characteristics between pitchup and pitchdown will persist. Much more in-depth investigation is required to reveal the physical mechanism for this hysteresis suppression phenomenon at high VR.

The present results, however, clearly show that increasing jet VR results in a higher value of achievable $C_{N\max}$ but does not significantly effect the value of $C_{M\max}$ (Fig. 7b). As with all of the previous experiments (for both pulsed and steady AJVG blowing), however, application of AJVG blowing results in a considerably higher pitching moment just before, and following, full stall on the pitchup, compared with the inactive jet or clean aerofoil cases.

In summary, it is suggested that a practical pulsed AJVG system should be designed to operate at a VR of at least 2.0. The results of this set of experiments confirm that increasing the jet-to-freestream VR, and thereby the blowing momentum coefficient C_μ, improves the performance of an AJVG system in effectively suppressing boundary-layer separation and delaying stall. It is therefore more important to maximize the jet velocity than the blowing mass flow rate.

D. Effect of Pulsing Frequency, $U = 35$ m/s and VR = 2.0

Figure 9 presents the variation of $C_{N\max}$ and $C_{T\max}$ with air-jet pulsing frequency for the case of a freestream wind speed of 35 m/s and a jet-to-freestream VR of 2.0. These data are obtained from the various pitch sweep experiments undertaken during the study, where the angle of attack is varied steadily while the tunnel freestream dynamic pressure is maintained constant.

It was found that there is a significant effect of pulsing frequency on the maximum achievable normal and tangential pressure forces. The optimum pulsing frequency for both C_N and C_T was found to be in the region of $F^+ = 0.6$–0.8, which agrees with the findings of Greenblatt and Wygnanski [28] and Greenblatt et al. [29,30].

Figure 10 presents the results of the tests performed to study the effect of varying the pulsing frequency with a constant jet VR of 2.0 and a freestream tunnel flow speed of 35 m/s at a fixed angle of attack, $\alpha = 22°$. Four tests were performed. Tests 1 and 3 started with a high frequency (250 Hz) and an attached leading-edge boundary layer, and they progressed by reducing the pulsing frequency, taking surface pressure readings at appropriate frequency increments. Tests 2 and 4 were similar, except that they began with a low frequency (2 Hz) and a fully separated leading-edge boundary layer, and they progressed by incrementally increasing the pulsing frequency. For each increment in pulsing frequency, the measured pressure distribution was integrated over the surface to yield the corresponding magnitude of normal force coefficient. Interestingly, there was a small difference between the data of Figs. 9 and 10, which indicate a sensitivity to the procedure used in the experiment. In the data for Fig. 10, where the angle of attack was constant, the only variable was pulsing frequency. Surface pressure distributions were carefully monitored to ensure that the correct physical starting conditions for the given test were achieved. With no changes in α, the disturbances during this experiment were significantly less than those with pitch variation.

The data for the constant α experiment (Fig. 10) clearly show that, despite a high degree of experimental scatter, a strong correlation between C_N and pulsing frequency is observed. For zero pulsing frequency (inactive jets), C_N is ~1.5, which is the value measured in previous tests of the inactive jet/clean surface model at $\alpha = 22°$. Under this condition, the upper-surface separation line was seen in the UV-tuft experiments to undergo transient switching between the fully separated flow case and the case where attachment was recovered on the forward 10% of the upper surface (see Fig. 11a). The periodicity in this switching between the two flow conditions was observed to be between 5 and 10 s. It is suggested that, at $\alpha = 22°$, the leading-edge boundary layer is extremely sensitive to external disturbances, and the flow switches between two bistable states in response to the level of freestream turbulence.

Switching on the pulsed air jets at a frequency of 2 Hz resulted in a significant change in the transients observed during the UV-tuft visualization experiments. The forward 10% of the upper surface was

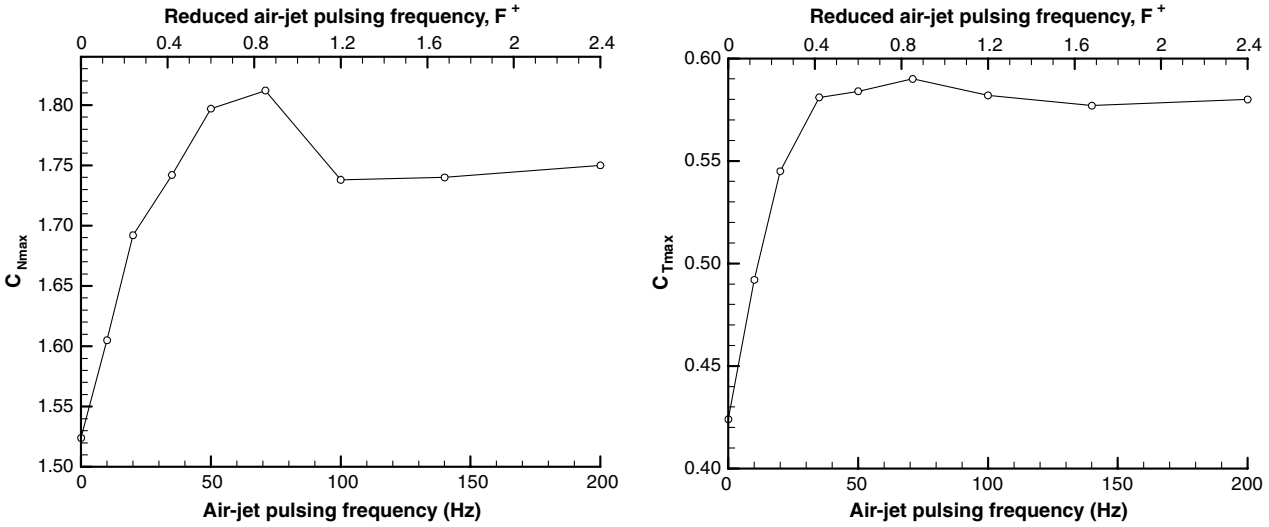

a) Maximum C_N **b) Maximum C_T**

Fig. 9 The effect of jet pulsing frequency on the maximum achievable normal and tangential force coefficient ($U = 35$ m/s and VR = 2.0).

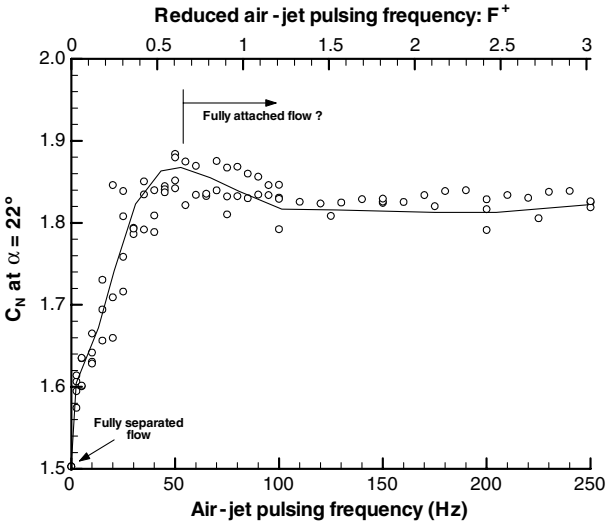

Fig. 10 Variation of normal force coefficient with AJVG pulsing frequency for the RAE 9645 section model for an angle of attack of 22°, VR = 2.0, and $U = 35$ m/s.

seen to become steadily attached, indicating that leading-edge suction had been permanently reestablished. However, downstream of the jets, the tufts were seen to respond in a wavelike manner to the activation of the AJVGs (Fig. 11c). When the jets were off, the separation line appeared to advance to a position just downstream of the jet array. When the jets were activated, the blowing appeared to force the separation line to retreat back downstream to a position of $x/c \approx 0.5$. The separation line was, in this way, clearly seen to advance and retreat in synchronization with the activation of the pulsed air jets. Analysis of the integrated C_N measurements undertaken at this condition indicate that, with the reestablishment of leading-edge suction, the normal force increased to between 1.57–1.61 by the activation of pulsing at 2 Hz. Further increases in pulsing frequency were observed in the UV-tuft experiments to increase the frequency at which the wavelike advance and retreat of the separation line occurred. The tuft technique was not able to resolve any small movements in the location of farthest extent, downstream or upstream, of the advancing–retreating separation line. However, the movement was clearly seen to remain in synchronization with the activation of the air jets.

At between $f = 40$–50 Hz, however, a different situation was observed in the response of the UV tufts. The rapid wavelike advance–retreat of the upper-surface separation line was no longer observed, and the separation line appeared to remain fixed at the downstream position. The maximum frame rate of the video camera prevented meaningful analysis at these high pulsing frequencies.

Analysis of the calculated C_N (Fig. 10) appears to show that a maximum value of $C_N \approx 1.85$–1.9 is achieved at around $f = 50$–70 Hz ($F^+ = 0.6$–0.8). For frequencies above 100 Hz, C_N was found to stabilize at an average value of 1.82. It is important to remember that, with the exception of the inactive jet case, the mass flow rates and the jet VR were constant for all pulsing frequencies, and the observed variation in C_N was purely frequency dependent. The two tests (1 and 3) performed, progressing from high jet pulsing frequency to low, further confirmed these findings, with the data following the same broad trends (Fig. 10 presented the combined data from all four of these tests).

As part of this set of experiments, dynamic pressure measurements at the trailing edge of the model, at $\alpha = 22°$, were recorded for the case of the clean aerofoil (sealed orifices) in an attempt to measure the natural shedding frequency of the RAE 9645 model at this angle of attack. This was done in order to investigate any link between the pulsing frequency, $f = 50$–70 Hz, at which maximum C_N is measured, and a change in flow physics is inferred in the experimental data. Analysis of the power density spectrum obtained during a vertical traverse through the wake, 10 mm offset downstream from the trailing edge, clearly identified a very strong dominant pressure fluctuation at about 45 Hz when the dynamic pressure sensor entered into the wake region, which was not present in the freestream. The assumption can confidently be made that this is associated with natural vortex shedding from the aerofoil. A similar analysis was performed for $U = 30$ m/s, where vortex shedding appeared to take place at a frequency of about 35 Hz. For both cases

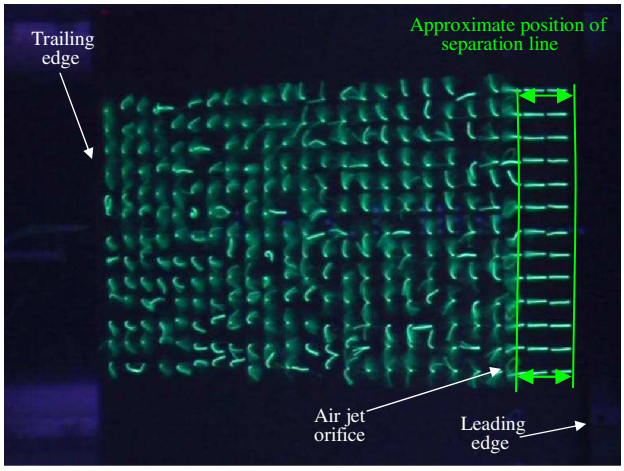

a) Inactive air jets

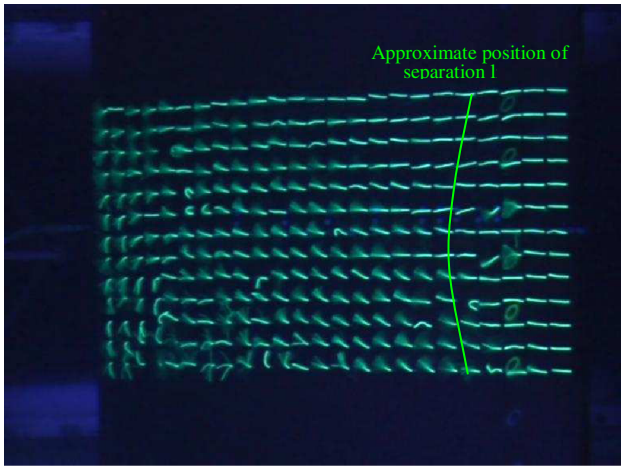

b) Steady air jets, VR=2.0

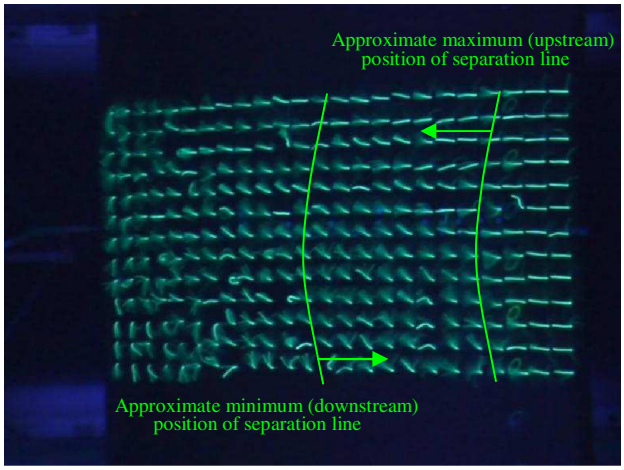

c) Pulsed air jets, VR=2.0, $f = 30$Hz

Fig. 11 Comparison of instantaneous surface flow visualization images of UV tufts on the upper surface of the RAE 9645 section model for $\alpha = 22°$ and $U = 35$ m/s.

of $U = 35$ m/s and $U = 30$ m/s, the Strouhal number associated with the shedding frequency was found to be about 0.6 for both cases. This corresponds with the value for the Strouhal number of 0.5–0.7 found in literature for aerofoils of low to moderate thickness-to-chord ratios.

Analysis of Fig. 10 shows that maximum C_N is achieved with an F^+ of ~0.6. This suggests that there is a lock-in effect between natural shedding frequency and the driving frequency of the AJVGs. However, experiments have only been performed for $U = 35$ m/s and VR = 2.0 at $\alpha = 22°$, where the flow is known to be particularly sensitive to pulsing frequency. To gain a more in-depth understanding of the physics behind pulsed AJVG blowing, and specifically the effect of pulsing frequency on the flow physics, a more in-depth set of experiments are required, covering different tunnel flow speeds and jet VRs, as well as the generation of more data for each condition.

In summary, there appears to be a clear correlation between jet pulsing frequency and the stall suppression effectiveness for a given jet VR and freestream tunnel speed. The optimum frequency also appears to be equivalent to the local natural shedding frequency of the aerofoil. A practical pulsed AJVG flow control system can therefore be effectively tuned to the local flow conditions to achieve the optimum stall suppression effect.

V. Conclusions

This experimental investigation aimed to conduct extensive tests, applying low-momentum steady and unsteady air injection on a RAE 9645 rotor blade section in a nominally two-dimensional flow, using pitched and skewed AJVGs to suppress quasi-steady flow separation and/or promote flow reattachment at low speeds. Results from this investigation have led to the following conclusions:

1) Hysteresis between the pitchup (continuous increase in angle of attack from $\alpha = -10°$ to a maximum of 26°) and the pitchdown (continuous decrease in angle of attack) data was evident in the normal and pitching-moment coefficients for jet-to-freestream VRs of 1.0, 1.5, 1.75, 2.0, and 2.5. No similar hysteresis phenomenon was observed for the highest jet velocity case, VR = 2.8, or in the data for the clean model data.

2) Steady AJVG blowing at a VR of 1.0, equal to the local freestream velocity, was ineffective in delaying the onset of trailing-edge separation, while a higher jet blowing velocity with VR = 2.0 delayed the onset of trailing-edge separation to a 2 to 3° higher angle of attack.

3) Unsteady AJVG blowing at a VR = 2.0, at pulsing frequencies equal to or above ~45–50 Hz, led to a ~20% increase in the maximum normal force over the clean aerofoil case, while steady AJVG blowing with an equivalent amount of total mass flow led only to a ~5% increase in the maximum normal force.

4) Unsteady AJVG blowing at or above ~45–50 Hz showed similar suppression of drag divergence (about 2° compared with inactive jets) as steady blowing but using half the total blowing mass flow, while low-frequency pulsing at 10 Hz was much less effective.

5) A correlation was found between aerofoil shedding frequency and maximum normal force, where a maximum normal force coefficient was obtained at about 45–50 Hz, corresponding to the measured natural shedding frequency. It is suggested that there is a tuning effect between natural shedding frequency and the driving frequency of the AJVGs. Although more extensive dynamic measurements of aerofoil shedding frequency are necessary in order to completely verify this.

6) The tufts detected periodic transient switching between fully separated and semiattached flow on the aerofoil upper surface at stalled flow conditions. This was believed to be low- frequency oscillations induced by unsteadiness in the freestream wind. The separation front was seen to advance upstream and retreat back downstream in a wavelike manner, in synchronization with the activation of the pulsed AJVGs at low frequencies (below ~5 Hz). The oscillations increased with increasing jet pulsing frequency.

7) The rapid wavelike advance–retreat of the upper-surface separation front was no longer observed at the higher frequencies of 40–50 Hz, close to the measured natural shedding frequency, and the separation front appeared to remain almost fixed, although this observation has to be fully verified with high-speed cameras in future studies.

Acknowledgments

This work was funded and supported by the U.K. Ministry of Defence and Department of Trade and Industry, as well as Augusta–Westland, Ltd., and QinetiQ, Ltd. The work was supported at City University by Chris Barber, Mike Smith, and Tim Barnes.

References

[1] Taylor, D. H., and Hoadley, H. H., "Application of Vortex Generator Mixing Principle to Diffusers," United Aircraft Corp. Rept. R-15064-5, East Hartford, CT, 1948.

[2] Wallis, R. A., "The Use of Air Jets for Boundary Layer Control," Aeronautical Research Labs., Aero. Note 110, Melbourne, Australia, 1952.

[3] Pearcey, H. H., "Shock Induced Separation and its Prevention by Design and Boundary Layer Control," *Boundary Layer and Flow Control*, edited by G. V. Lachmann, Pergamon, New York, 1961, pp. 1166–1134.

[4] Freestone, M., "Preliminary Tests at Low Speeds on the Vorticity Produced by Air-Jet Vortex Generators," City University, Department of Aeronautics Research Memo. 85/1, London, Feb. 1985.

[5] Pauley, W. R., and Eaton, J. K., "Experimental Study of the Development of Longitudinal Vortex Pairs Embedded in a Turbulent Boundary Layer," *AIAA Journal*, Vol. 26, No. 7, 1988, pp. 816–823. doi:10.2514/3.9974

[6] Johnston, J. P., and Nishi, M., "Vortex Generator Jets: A Means of Flow Separation Control," AIAA Paper 1989-0564, 1989.

[7] Selby, G. V., Lin, J. C., and Howard, F. G., "Control of Low-Speed Turbulent Separated Flow Using Jet Vortex Generators," *Experiments in Fluids*, Vol. 12, No. 6, 1992, pp. 394–400. doi:10.1007/BF00193886

[8] Compton, D. A., and Johnston, P., "Streamwise Vortex Production by Pitched and Skewed Jets in a Turbulent Boundary Layer," *AIAA Journal*, Vol. 30, No. 3, 1992, pp. 640–647. doi:10.2514/3.10967

[9] Henry, F. S., and Pearcey, H. H., "Numerical Model of Boundary Layer Control Using Air-Jet Generated Vortices," *AIAA Journal*, Vol. 32, No. 12, 1994, pp. 2415–2424. doi:10.2514/3.12308

[10] Zhang, X., and Collins, M. W., "Measurements of a Longitudinal Vortex Generated by a Rectangular Jet in a Turbulent Boundary Layer," *Physics of Fluids*, Vol. 9, No. 6, 1997, pp. 1665–1673. doi:10.1063/1.869286

[11] Zhang, X., and Collins, M. W., "Nearfield Evolution of a Longitudinal Vortex Generated By Inclined Jet in a Turbulent Boundary Layer," *Journal of Fluids Engineering*, Vol. 119, No. 4, Dec. 1997, pp. 934–939. doi:10.1115/1.2819520

[12] Singh, C., Peake, D. J., Coton, F., Kokkalis, A., Khodagolian, V., Coton, F., and Galbraith, R. A., "Parametric Study of an Air-Jet Vortex Generator Configuration to Control Rotorcraft Retreating Blade Stall," 43rd AIAA Aerospace Sciences Meeting and Exhibit, Reno, NV, AIAA Paper 2005-1366, 10–13 Jan. 2005.

[13] Singh, C., "Application of Airjet Vortex Generators To Control Helicopter Retreating Blade Stall," Ph.D. Dissertation, City University London, 2006.

[14] Oyler, T. E., and Palmer, W. E., "Exploratory Investigation of Pulsed Blowing for Boundary Layer Control," North American Rockwell Corp. Rept. NR 72H-12, 1972.

[15] Oster, D., Wygnanski, I., Dziomba, B., and Fiedler, H., "On the Effect of Initial Conditions on the Two Dimensional Turbulent Mixing Layer," *Lecture Notes in Physics*, Vol. 75, 1978, pp. 48–64. doi:10.1007/3-540-08765-6_5

[16] Oster, D., and Wygnanski, I., "The Forced Mixing Layer Between Parallel Streams," *Journal of Fluid Mechanics*, Vol. 123, 1982, pp. 91–130. doi:10.1017/S0022112082002973

[17] Wygnanski, I., and Pedersen, R. A., "Coherent Motion in Excited Free Shear Flows," *AIAA Journal*, Vol. 25, No. 2, 1987, pp. 201–213. doi:10.2514/3.9610

[18] Ho, C. M., and Huerre, P., "Perturbed Free Shear Layers," *Annual Review of Fluid Mechanics*, Vol. 16, No. 1, 1984, pp. 365–422.

doi:10.1146/annurev.fl.16.010184.002053
[19] Katz, Y., Nishri, B., and Wygnanski, I., "The Delay of Turbulent Boundary Layer Separation by Oscillatory Active Control," *Physics of Fluids*, Vol. 1, No. 2, 1989, pp. 179–181. doi:10.1063/1.857555
[20] Seifert, A., Bachar, T., Koss, D., Shepshelovich, M., and Wygnanski, I., "Oscillatory Blowing: A Tool to Delay Boundary Layer Separation," *AIAA Journal*, Vol. 31, No. 11, 1993, pp. 2052–2060. doi:10.2514/3.49121
[21] McManus, K. R., Ducharme, A., Goldley, C., and Magill, J., "Pulsed Jet Actuators for Suppressing Flow Separation," 34th AIAA Aerospace Sciences Meeting and Exhibit, Reno, NV, AIAA Paper 1996-0442, Jan. 1996.
[22] McManus, K. R., Legner, H. H., and Davis, S. J., "Pulsed Vortex Generator Jets for Active Control of Flow Separation," 25th AIAA Fluid Dynamics Conference, Colorado Springs, CO, AIAA Paper 1994-2218, June 1994.
[23] Seifert, A., Darabi, A., and Wygnanski, I., "Delay of Airfoil Stall by Periodic Excitation," *Journal of Aircraft*, Vol. 33, No. 4, 1996, pp. 691–698. doi:10.2514/3.47003
[24] McManus, K. R., Joshi, P. B., Legner, H. H., and Davis, S. J., "Active Control of Aerodynamic Stall Using Pulsed Jet Actuators," 26th AIAA Fluid Dynamics Conference, AIAA Paper 1995-2187, June 1995.
[25] McManus, K. R., Ducharme, A., Goldey, C., and Magill, J., "Pulsed Jet Actuators for Suppressing Flow Separation," 34th Aerospace Sciences Meeting and Exhibit, Reno NV, AIAA Paper 1996-0442, Jan. 1996.
[26] McManus, K. R., and Magill, J., "Separation Control in Incompressible and Compressible Flow Using Pulsed Jets," AIAA Paper 1996-1948, June 1996.
[27] Magill, J. C., and McManus, K. R., "Control of Dynamic Stall Using Pulsed Vortex Generator Jets," 36th Aerospace Sciences Meeting and Exhibit, Reno, NV, AIAA Paper 1998-0675, 1998.
[28] Greenblatt, D., and Wygnanski, I., "Dynamic Stall Control by Oscillatory Addition of Momentum. Part 1: NACA 0015 Parametric Study," *Journal of Aircraft*, Vol. 38, No. 3, 2001, pp. 430–438. doi:10.2514/2.2810
[29] Greenblatt, D., Nishri, B., Darabi, A., and Wygnanski, I., "Dynamic Stall Control by Oscillatory Addition of Momentum. Part 2: Mechanisms," *Journal of Aircraft*, Vol. 38, No. 3, 2001, pp. 439–447. doi:10.2514/2.2811
[30] Greenblatt, D., "Dual Location Separation Control on a Semispan Wing," *AIAA Journal*, Vol. 45, No. 8, 2007, pp. 1848–1860. doi:10.2514/1.27757
[31] Eroglu, A., and Breidental, R. E., "Structure, Penetration and Mixing of Pulsed Jets in Crossflow," *AIAA Journal*, Vol. 39, No. 3, 2001, pp. 417–423. doi:10.2514/2.1351
[32] Johari, H., "Scaling of Fully Pulsed Jets in Crossflow," *AIAA Journal*, Vol. 44, No. 11, 2006, pp. 2719–2725. doi:10.2514/1.18929
[33] Scholz, P., Casper, M., Ortmanns, J., Kähler, C., and Radespiel, R., "Leading-Edge Separation Control by Means of Pulsed Vortex Generator Jets," *AIAA Journal*, Vol. 46, No. 4, April 2008, pp. 837–846. doi:10.2514/1.26176
[34] Ortmanns, J., Bitter, M., and Kahler, C. J., "Dynamic Vortex Structures for Flow-Control Applications," *Experiments in Fluids*, Vol. 44, No. 3, 2008, pp. 397–408. doi:10.1007/s00348-007-0442-8
[35] Jones, B. M., "The Measurement of Profile Drag by the Pitot Traverse Method," Aeronautical Research Council Rept. 1688, 1936.

F. Coton
Associate Editor